Supporting Information

2D Auxetic Material with Intrinsic Ferromagnetism: Copper Halide ($CuCl_2$) Monolayer

Haifei Qin,[a] Jiao Chen,[a] Bai Sun,[a] Yongliang Tang,[a] Yuxiang Ni,[a] Zhongfang Chen[b,*] Hongyan Wang,[a] and Yuanzheng Chen,[a, c, d,*]

[a] *School of Physical Science and Technology, Key Laboratory of Advanced Technologies of Materials, Ministry of Education of China, Southwest Jiaotong University, Chengdu 610031, China*
[b] *Department of Chemistry, University of Puerto Rico, Rio Piedras Campus, San Juan, PR 00931, USA.*
[c] *Beijing Computational Science Research Center, Haidian District, Beijing 100193, China*
[d] *Department of Physics and Centre for Advanced Two-Dimensional Materials, National University of Singapore, Singapore 117551 Singapore*

Details of structure prediction

The particle swarm optimization (PSO) method within the evolutionary algorithm as implemented in the CALYPSO[1, 2] code was employed to find the lowest energy structures of Cu_xCl_{1-x} monolayer (x = 2/3, 1/2, 3/7, 2/5, 1/3, 1/4 and 1/5). Unit cells containing 1, 2, 3, and 4 formula units (f.u.) were considered. Structure searches for the Cu-Cl compound were performed at 0 and 10 GPa. In the first step, random structures with certain symmetry are constructed in which atomic coordinates are generated by the crystallographic symmetry operations. Local optimizations using the VASP code[3] were done with the conjugate gradients method and terminated when the Gibbs free energy converged with changes smaller than 1×10^{-6} eV per cell. After processing the first-generation structures, 60% of them with lower Gibbs free energies were selected to construct the next generation structures by PSO. 40% of the structures in the new generation were randomly generated. A structure fingerprinting technique with bond characterization matrix was applied to the generated structures, so that identical structures are strictly forbidden. These procedures significantly enhance the diversity of the structures, which is crucial for structural global search efficiency. In most cases, structural searching simulations for each calculation were stopped after generating 1000 ~ 1200 structures (e.g., about 20 ~ 35 generations).

Phonon calculations were performed for $6 \times 6 \times 1$ supercell for $CuCl_2$ by using a supercell approach with the finite displacement method as implemented in the Phonopy code[4]. The strain is defined as , where and $\varepsilon = (a - a_0)/a_0 \times 100\% = (b - b_0)/b_0 \times 100\%$ a, b, a_0, b_0 are the lattice constants of the unit cell under strain and at equilibrium, respectively.

Supporting Figures

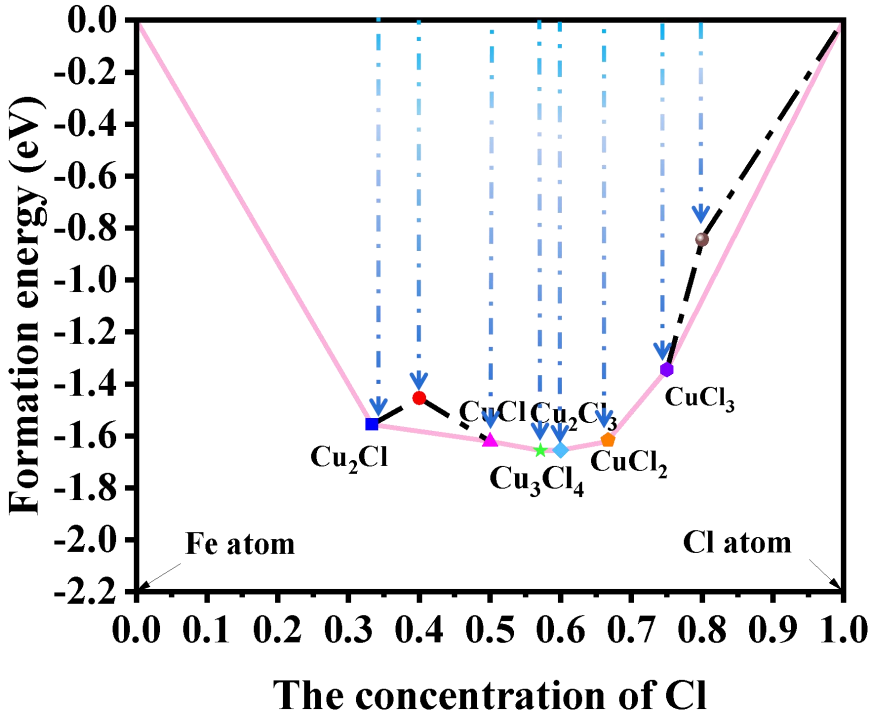

Figure S1. Computed formation energy vs the chlorine concentration for the Cu−Cl monolayers. The convex hull is labeled by the pink solid line.

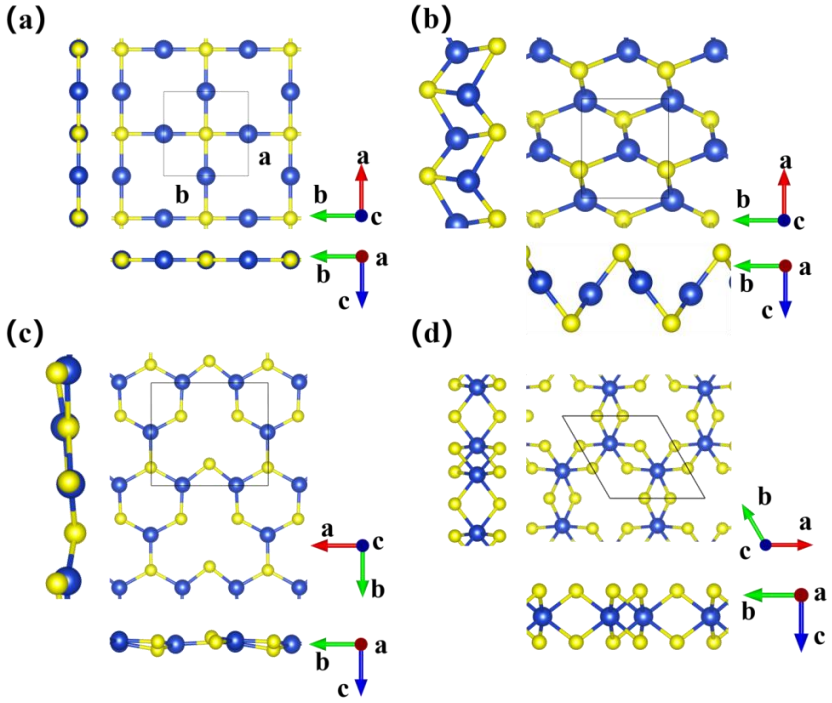

Figure S2. The structure of (a) Cu_2Cl, (b) CuCl, (c) Cu_3Cl, (d) $CuCl_3$ from the side, top, and front views. The yellow and blue atoms represent Cl and Cu atoms.

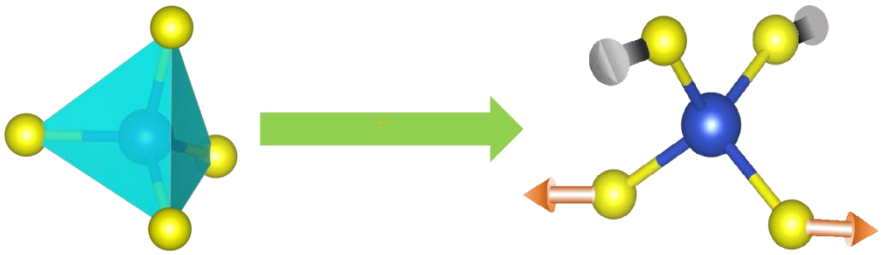

Figure S3. The explanation of Poisson's ratio for our new 2D $CuCl_2$ monolayer. Each Cu atom is surrounded by four Cl atoms and due to its shape each $CuCl_4$ group is called $CuCl_4$ tetrahedron. when the tensile strain is applied to the edge to the tetrahedron (vertical to 2-fold axis), similarly because of the angular variation the distance of two Cl atoms increases, leading a NPR phenomenon.

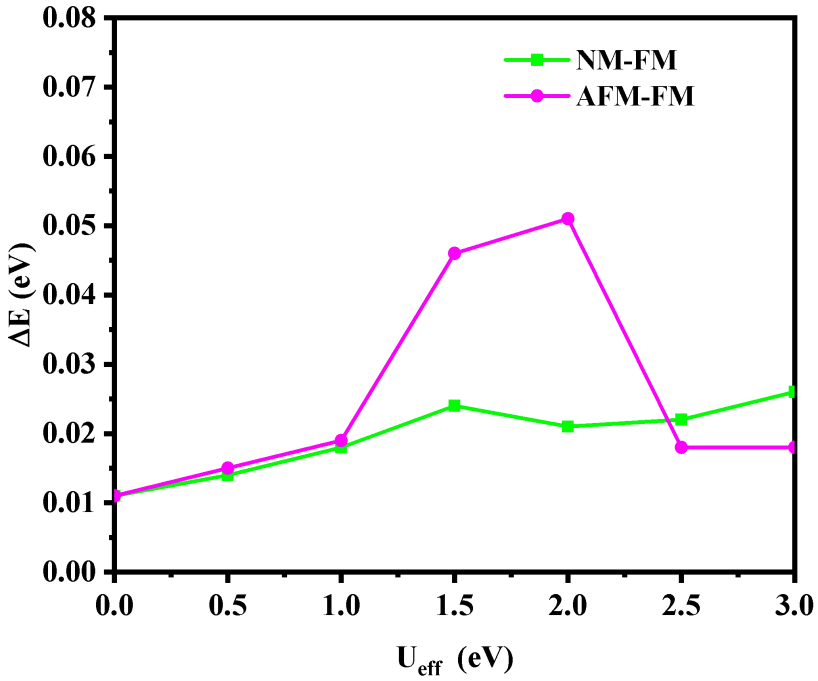

Figure S4. The energy differences of different states (NM, FM, AFM) for the $CuCl_2$ monolayer as a function of U_{eff}.

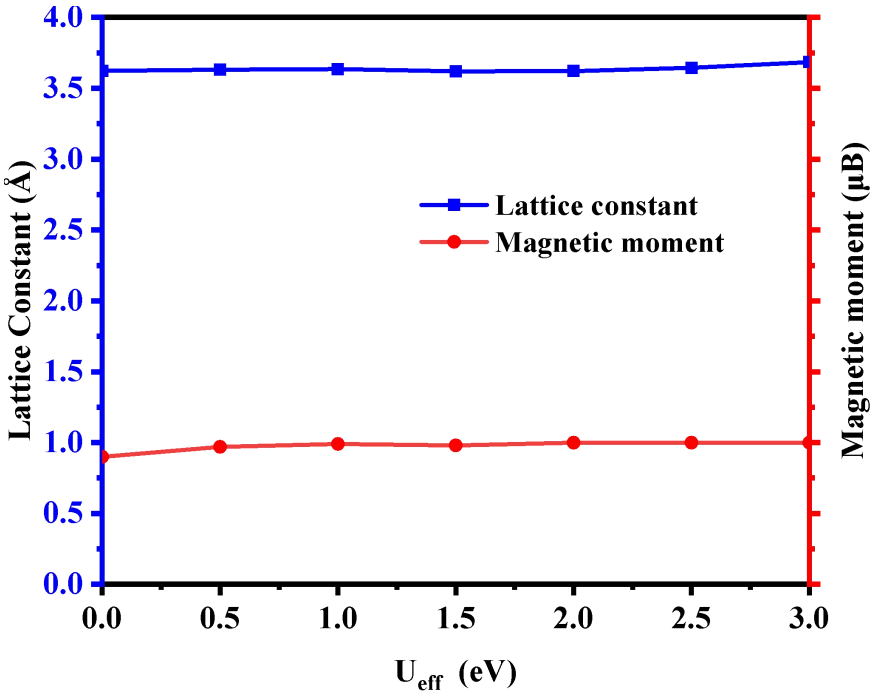

Figure S5. Lattice constants and magnetic moment of the $CuCl_2$ monolayer as a function of U_{eff}.

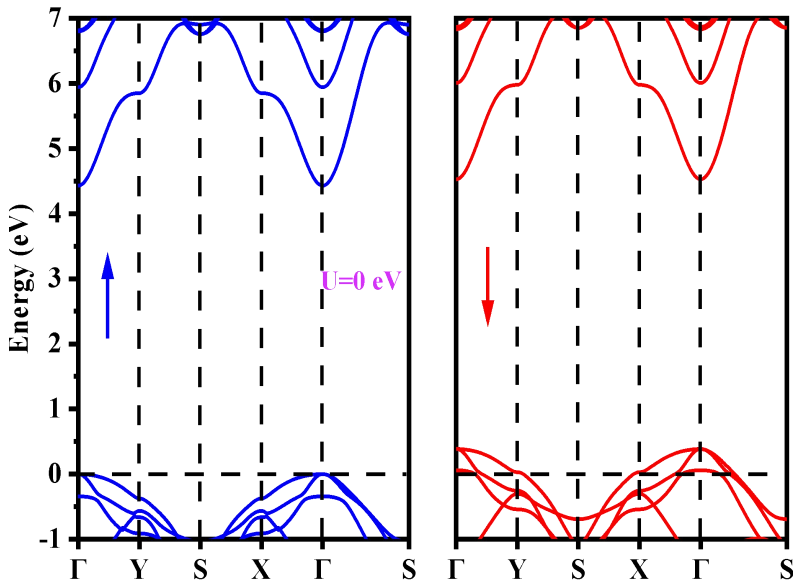

Figure S6. Band Structure of $CuCl_2$ monolayer calculated using standard GGA_PBE level (U=0).

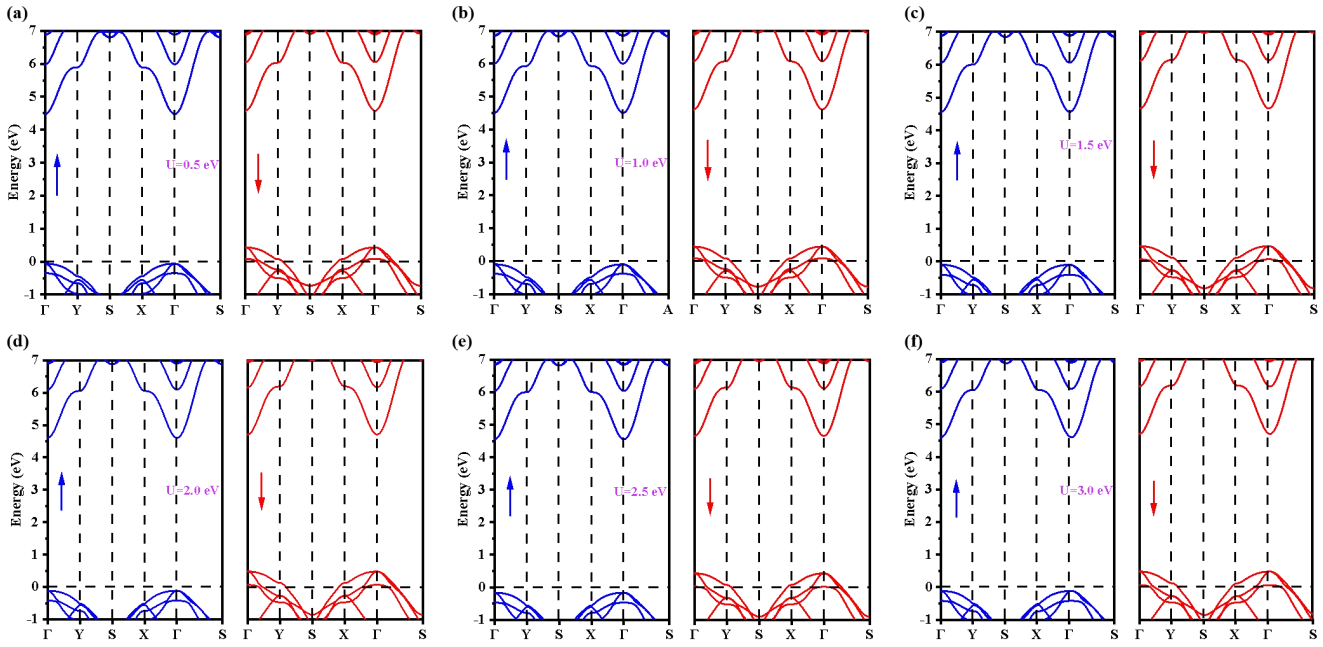

Figure S7. Band Structure of $CuCl_2$ monolayer calculated using GGA+U method with U_{eff} value of (a) 0.5 eV, (b) 1 eV, (c) 1.5 eV, (d) 2 eV, (e) 2.5 eV and (f) 3 eV.

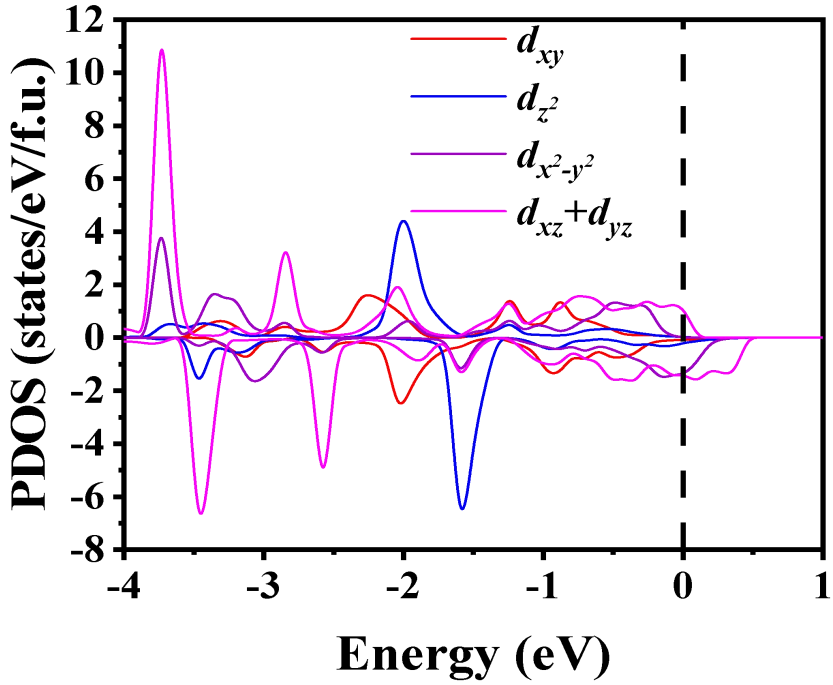

Figure S8. The Cu-d spin orbital projected density of states for $CuCl_2$ monolayer under the symmtry of D_{2d}.

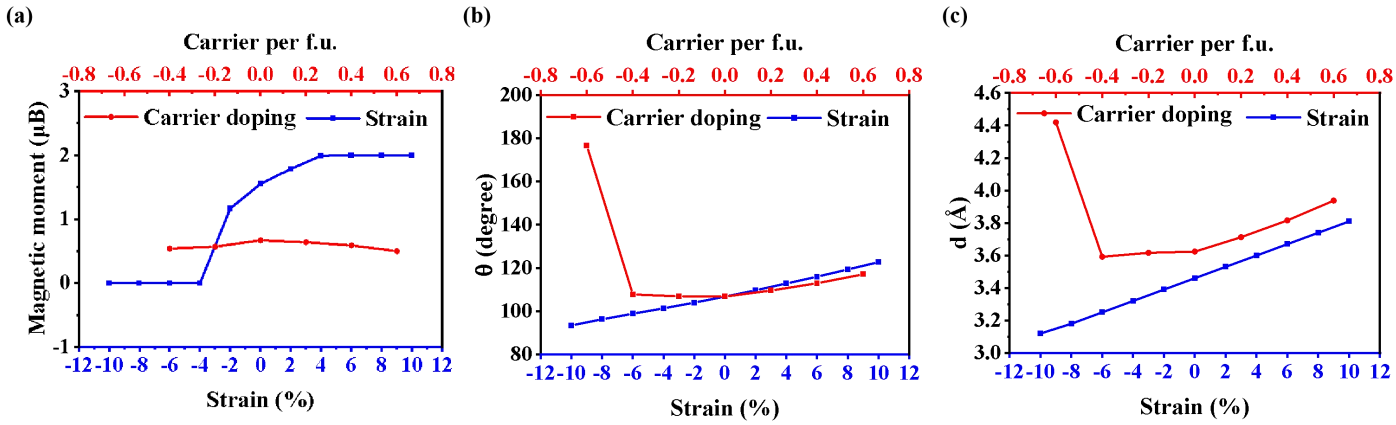

Figure S9. The (a) magnetic moment, (b) Cu-Cl-Cu angle and (c) Cu-Cu distance of $CuCl_2$ monolayer under the biaxial strain and carrier doping.

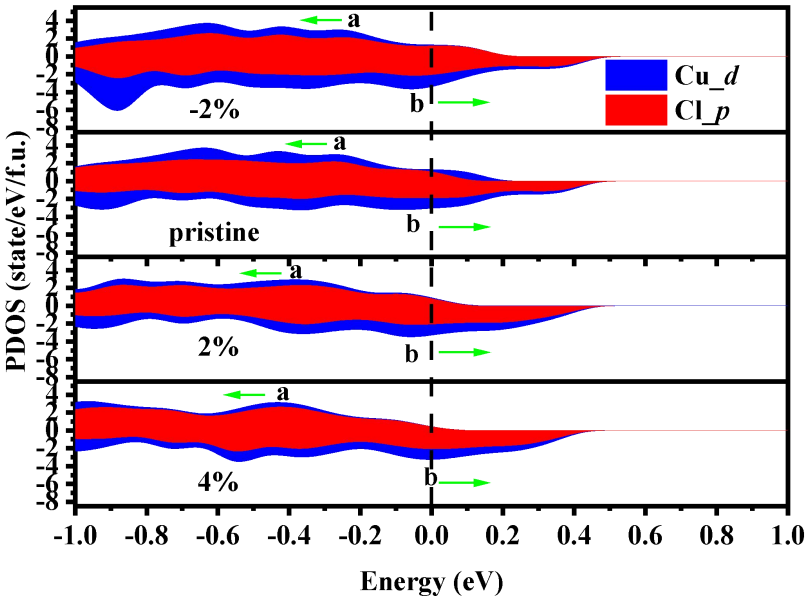

Figure S10. Partial spin density of states (PDOS) for the -2%, pristine, 2% and 4% $CuCl_2$ monolayer under the ground state. We can observe the spin splitting of the a and b states in PDOS.

Supporting Tables

Table S1. The more specific details of $CuCl_2$ monolayer.

phase	Space group	a (Å)	b (Å)	c (Å)		ΔE (eV)	Thickness (Å)	bond length (Å)	Cu-Cl-Cu band angle (degree)	Cl-Cu-Cl band angle (degree)
$CuCl_2$	*P-4/m2*	3.62	3.62	18.31	$\alpha=\beta=\gamma=90°$	-1.62	2.75	2.26	106.80	110.82

References

1. Y. Wang, J. Lv, L. Zhu and Y. Ma, *Phys. Rev. B.*, 2010, **82**, 094116.
2. Y. Wang, J. Lv, L. Zhu and Y. Ma, *Comput. Phys. Commun.*, 2012, **183**, 2063-2070.
3. G. Kresse and J. Furthmüller, *Phys. Rev. B.*, 1996, **54**, 11169-11186.
4. D. Xiao, G.-B. Liu, W. Feng, X. Xu and W. Yao, *Phys. Rev. Lett.*, 2012, **108**, 196802.